ELSEVIER

Earth and Planetary Science Letters 192 (2001) 363–376

EPSL

www.elsevier.com/locate/epsl

Ar diffusion in hydrous silicic melts: implications for volatile diffusion mechanisms and fractionation

Harald Behrens [a,*], Youxue Zhang [b]

[a] Institut für Mineralogie, Universität Hannover, Welfengarten 1, D-30167 Hannover, Germany
[b] Department of Geological Sciences, University of Michigan, Ann Arbor, MI 48109-1063, USA

Received 2 May 2001; received in revised form 17 July 2001; accepted 26 July 2001

Abstract

The effect of dissolved water on the diffusivity of Ar in glasses and melts of rhyolitic and albitic compositions was investigated experimentally at pressures up to 1500 MPa and water contents of 0.1–5 wt%. The data for water-poor rhyolitic composition at 500 MPa can be described in the whole temperature range of 480–1102°C by a simple Arrhenius relationship $D_{Ar} = 2.14 \times 10^{-6}$ m^2/s exp($-18\,883/T$). A 4.0 wt% increase in water content increases the Ar diffusivity by approximately one order of magnitude in both rhyolitic and albitic melts at 1000°C. In contrast to viscosity and total water diffusion, an exponential dependence of Ar diffusivity on water content was observed for the rhyolitic composition in the whole range of water contents. For water-poor rhyolite, Ar diffusivity depends on pressure with an apparent activation volume of 13–15 cm^3/mol at pressures up to 800 MPa. For water-rich rhyolite ($\sim$5 wt% water), there is no significant pressure effect at 1000°C in the range 500–1500 MPa. Combining our data with previous data from Carroll [M.R. Carroll, Earth Planet. Sci. Lett. 103 (1991) 156–168], Ar diffusivity (in 10^{-12} m^2/s) in rhyolitic melts can be expressed as:

$$D_{Ar} = \exp[(14.627 - 17913/T - 2.569P/T) + (35936/T + 27.42P/T)X_{water}]$$

where T is in K, P in MPa, and X_{water} is the mol fraction of water on a single oxygen basis. Except for two outlier points, error of estimates is ≤ 0.455 in terms of ln D for all data, covering a wide range of temperatures (480–1200°C), pressures (0.1–1500 MPa), and water contents (0.1–5 wt%). The new Ar diffusion data support the assumption that molecular H_2O diffusivity exponentially increases with water content [Y. Zhang, H. Behrens, Chem. Geol. 169 (2000) 243–262].

Keywords: argon diffusion; rhyolites; albite; melts; glasses; degassing

1. Introduction.

Knowledge of Ar diffusion in silicate melts is important to understanding the behavior of noble gases during degassing of magmas. The relative abundance of the noble gases in the magma after decompression and degassing depends on the solubilities and diffusivities of the noble gases in the

* Corresponding author. Tel.: +49-511-762-8054; Fax: +49-511-762-3504.
E-mail address: h.behrens@mineralogie.uni-hannover.de (H. Behrens).

0012-821X/01/$ – see front matter
PII: S0012-821X(01)00458-7

melt as well as on the degree of degassing. In a slowly ascending magma, equilibrium between the exsolved gas and the melt may be maintained and fractionation of the major, minor and noble gases depends on the initial gas concentrations and on the solubilities [2]. On the other hand, if the magma is rapidly decompressed during volcanic eruptions, kinetic fractionation will affect gas abundance due to the different diffusivities of the gases in the melts. In addition, Ar diffusion data may provide insight into the diffusion mechanisms of charged and uncharged particles in silicate melts. Systematic variation of the activation energy with particle size and charge was found for diffusion of noble gases, alkali and alkali earth elements in natural rhyolitic melts [3,4] as well as in simple synthetic melts [4–8].

Although most natural silicic melts contain dissolved water (up to 8 wt% in rhyolitic melts [9]), only few diffusion studies were performed on hydrous melts [10–12], and none was on noble gas diffusion. In this contribution we present new experimental results on Ar diffusion in water-bearing silica-rich melts, mainly rhyolitic composition. To elucidate whether the effect of dissolved water depends on the anhydrous composition, we have carried out a few additional experiments on albitic composition.

Another purpose of the new Ar diffusion data is to improve our understanding of the diffusion mechanisms of the major volatiles in magmas, water and carbon dioxide. Both of them dissolve in silicate melts in at least two forms, as unreacted molecular species (H_2O and CO_2 molecules) and as species such as hydroxyl groups and carbonate ion complexes formed by reaction between the molecular species and the silicate solvent. The diffusion of the individual species as well as the reaction between the species and the silicate network may influence the overall transport of these components in the melt. Modeling diffusion profiles of these components in quenched glasses can give insight into the importance of the individual species to the total flux of the component [13,14]. However, these conclusions are indirect. In the case of water diffusion, it has been suggested that molecular H_2O diffusivity depends exponentially on total water content [1]. Investigation of Ar diffusion can verify whether this assumption is reasonable because Ar, in contrast to water, is a simple atomic species and migrates by a simple mechanism involving atomic jumps through the silicate network.

2. Starting materials

2.1. Water-poor glasses

Natural rhyolitic glasses are from Mono Craters, CA, USA, and contain 0.1–2.0 wt% water. The glasses contain small amounts of microlites and bubbles but the effect of these on Ar diffusion results is expected to be negligible from results of water diffusion experiments [14]. The dry albitic glass was synthesized by Schott company (Mainz, Germany) and contains large vesicles 0.1–1 mm in size. Nevertheless, spacing between the vesicles (0.5–2 mm) is typically much larger than the length of Ar profiles so that one-dimensional diffusion conditions can be established in the experiments. Both the rhyolitic and albitic compositions were used in several previous studies, e.g. on water diffusion [1,14,15] and water speciation [16–19], so that the results on Ar diffusion can be directly compared with other melt properties. Compositions of the glasses are given in Table 1.

Table 1
Composition of glasses used in this study (wt%)

	KS rhyolite	EDF rhyolite	Ab albite
SiO_2	76.52	76.69	69.19
TiO_2	0.06	0.11	–
Al_2O_3	12.61	12.70	18.83
FeO_{total}	1.00	0.67	0.00
MgO	0.03	0.08	–
CaO	0.54	0.57	0.00
Na_2O	4.03	4.05	11.96
K_2O	4.79	4.77	0.02
H_2O_{total}	0.761	0.215	0.036
Sum	100.34	99.86	100.04

Major oxide contents were analyzed by electron microprobe. Water contents (H_2O_{total}) were determined from room temperature IR spectra. All iron is given as FeO_{total}.

Table 2
Ar diffusion data for rhyolitic and albitic melts

Exp. no.	app.	T (°C)	P (MPa)	Time nominal (s)	Time corrected (s)	Water initial (wt%)	Water final (wt%)	$C_{Ar,surface}$ measured/fit (wt%)	$C_{Ar,max}$ (wt%)	D_{Ar} (10^{-12} m^2/s)
Rhyolite										
KS-D24P[a]	CSPV	480	500	1 067 900	–	0.86	< 0.5	–/0.79	–	$(4.2 \pm 2.8) \times 10^{-5}$
KS-D23P[a]	CSPV	563	500	236 800	–	0.73	< 0.4	–/0.61	–	$(2.3 \pm 1.3) \times 10^{-4}$
KS-D13P[a]	CSPV	588	50	167 700	–	0.81	< 0.5	–/0.043	–	$(3.8 \pm 1.4) \times 10^{-3}$
KS-D18P[a]	IHPV	592	801	252 900	–	0.82	< 0.4	–/0.99	–	$(3.0 \pm 1.6) \times 10^{-4}$
KS-D19P[a]	CSPV	601	200	277 760	–	0.79	< 0.5	–/0.18	–	$(1.8 \pm 0.7) \times 10^{-4}$
KS-D12P[a]	CSPV	602	500	263 650	–	0.79	< 0.4	0.485/0.48	–	$(6.3 \pm 2.6) \times 10^{-4}$
Rhy-D12P[a]	CSPV	605	500	144 300	–	1.86	< 0.8	0.485/0.47	–	$(8.7 \pm 3.9) \times 10^{-4}$
SRhy-DAr1[a]	IHPV	907	500	36 000	–	0.22	< 0.21	0.36–0.53/0.44	–	0.27 ± 0.06
RhyAr12-0	IHPV	1 000	100	1 800	1 888	0.12	< 0.10	0.081/0.073	–	1.16 ± 0.25
RhyAr10-0	IHPV	1 000	100	14 400	–	0.12	< 0.10	–/0.11	–	1.31 ± 0.24
RhyAr11-0	IHPV	1 000	300	14 400	–	0.12	< 0.10	0.215/0.215	–	1.49 ± 0.27
SRhy-DAr2[a]	IHPV	1 025	500	14 400	–	0.22	< 0.19	0.50/0.43	–	1.41 ± 0.25
RhyAr3-4	IHPV	1 034	500	5 400	5 480	0.24	< 0.19	0.51/0.38	–	1.19 ± 0.22
RhyAr4-0	IHPV	1 102	500	1 800	1 888	0.24	< 0.22	–/0.43	–	2.14 ± 0.39
DCRhyAr6-2	IHPV	900	500	7 200	–	2.3/2.2	2.03/2.04/2.08	–	0.13	0.72 ± 0.22
DCRhyAr6-5	PCA	1 000	500	600	–	5.0/5.0	4.61/4.62/4.60	–	0.07	13.3 ± 4.0
DCRhyAr7-5	PCA	1 000	1 000	600	–	5.0/5.2	4.98/5.00/5.02	–	0.13	18.9 ± 5.7
DCRhyAr8-5	PCA	1 000	1 500	600	–	5.0/5.2	5.05/5.00/5.03	–	0.13	15.6 ± 4.7
DCRhyAr2-1	IHPV	1 025	500	14 400	–	0.9/0.9	0.88/0.90/0.88	–	0.11	2.08 ± 0.62
DCRhyAr3-1	IHPV	1 034	500	5 400	5 480	2.2/5.2	2.35/2.72/3.17	–	0.11	5.6 ± 2.2
DCRhyAr3-2	IHPV	1 034	500	5 400	5 480	2.2/3.7	3.16/3.46/3.66	–	0.14	9.7 ± 2.9
DCRhyAr3-3	IHPV	1 034	500	5 400	5 480	2.0/4.8	3.20/4.01/4.44	–	0.21	20.1 ± 8.0
DCRhyAr4-1	IHPV	1 102	500	1 800	1 888	0.9/0.9	0.88/0.90/0.92	–	0.11	3.8 ± 1.2
DCRhyAr4-2	IHPV	1 102	500	1 800	1 888	2.2/2.3	2.00/2.04/2.11	–	0.11	8.9 ± 2.7
DCRhyAr4-4	IHPV	1 102	500	1 800	1 888	3.8/4.0	3.81/3.87/3.95	–	0.10	24.1 ± 7.2
DCRhyAr4-x	IHPV	1 102	500	1 800	1 888	2.0/4.8	3.14/3.96/4.48	–	0.10	21.8 ± 8.7
DCRhyAr5-1	IHPV	1 198	500	1 200	1 482	0.9/0.9	0.91/0.92/0.93	–	0.11	7.1 ± 2.1
DCRhyAr5-2	IHPV	1 198	500	1 200	1 482	2.4/2.2	2.18/2.11/2.06	–	0.11	14.6 ± 4.4
DCRhyAr5-4	IHPV	1 198	500	1 200	1 482	4.1/3.7	4.05/4.04/3.96	–	0.11	37.3 ± 11.2
Albite										
AbD12P	CSPV	605	500	65 340	–	1.85	< 0.9	0.245	–	$(5.2 \pm 3.3) \times 10^{-4}$
AbDAr1	IHPV	903	500	36 000	–	0.036	< 0.050	0.27/0.27	–	0.21 ± 0.06
AbDAr2	IHPV	1 015	500	14 400	–	0.036	< 0.055	0.265/0.305	–	1.27 ± 0.23
DCAbDAr2	IHPV	1 015	500	14 400	–	4.3/4.1	4.25/4.25/4.23	–	0.021	10.5 ± 3.1

Water concentrations in diffusion couples are given at $x+2(D_{Ar}t)^{1/2}/x/x-2(D_{Ar}t)^{1/2}$ where x is the Matano interface of the Ar profile. Maximum water contents, measured either near the surface (AbDAr1 and AbDAr2) or at the end of the Ar profile (all other samples) are given for sorption experiments.
[a]Sample from water diffusion study of Zhang and Behrens [1].

2.2. Synthesis of hydrous glasses

Hydrous Ar-bearing glasses were produced in two ways.

1. Rhyolitic glass powder with grain size <200 μm was annealed for 2 h in an open Au capsule at 800°C, 300 MPa in a cold seal pressure vessel (CSPV) using Ar as the pressure medium. The Ar content of the resulting glass was in average 0.23 wt% as measured by electron microprobe analysis of several individual grains. Ar-free and Ar-bearing glass powders were mixed in a 2:1 ratio to get an Ar content of the diffusion samples of about 0.1 wt%. To produce hydrous glasses, glass powder and doubly distilled water were loaded in Au capsules in several portions by turns. After welding shut, syntheses were performed in an internally heated gas pressure vessel (IHPV) at 1000°C and 500 MPa for 2–3 days.

2. Hydrous albitic glass powder (with 4.1 wt% water determined by Karl-Fischer titration) was filled into a large Pt capsule and the capsule was flushed at 1 atm with Ar gas before welding shut. The capsule was processed in an IHPV at 1200°C, 500 MPa for 2 days to dissolve and homogenize Ar in the glass.

All hydrous glasses contain small bubbles (up to 20 μm in diameter) which are inhomogeneously distributed in the glasses and which vary widely in size. Because the appearance of the bubbles is not related to the Ar and H_2O concentration (i.e. bubbles are observed in both Ar-free and Ar-bearing glasses) we attribute the bubbles to air enclosed in the capsule during preparation. The volume fraction of bubbles was always very small (0.1–0.2 vol%, estimated by counting the number of bubbles in polished sections 0.1 mm thick using an optical microscopy) and we do not expect a significant influence of them on the diffusion results.

3. Experimental procedures

3.1. Ar sorption experiments

Most of these experiments were designed to study water diffusion [1]. Ar diffusivities were obtained as a byproduct. A detailed description of these runs is given by Zhang and Behrens [1]. At low temperature runs were conducted in rapid-quench CSPV (except for one high pressure experiment) and at high temperatures in vertical IHPVs (Table 2). Doubly polished plates (typical size $4\times4\times1$ mm) of water-poor glass were loaded in open Au capsules or simply wrapped in Au foil. During the run, samples are directly exposed to the pressure medium Ar. Water diffuses out of the sample and Ar diffuses into the sample. The temperature uncertainty at the sample position is estimated to be 10°C and temperature gradient is less than 1°C/mm. The pressure of the CSPV and the IHPV was automatically controlled to within 5 MPa during the experiment and during quench (cooling rates of 30°C/s in the CSPV [20] and 100°C/min in the IHPV (measured).

3.2. Diffusion couple experiments

Each diffusion couple consists of two hydrous glass cylinders (2 mm in length, 3 mm in diameter), one Ar-bearing and one Ar-free. The glass cylinders were polished on both base surfaces and the water content of each cylinder was determined by near-infrared spectroscopy before the experiment. The two halves of the couple were placed together in a platinum capsule so that the polished surfaces were in contact. The capsule was manually squeezed to minimize air and free space in the capsule, welded shut, and compressed in Ar gas at room temperature in a CSPV. The compressed capsule was then placed in an IHPV or in a piston cylinder apparatus (PCA), pressurized, and heated to the experimental temperature for a specific duration. Run conditions in the IHPV were the same as those described above for sorption experiments. For the PCA experiments, the cell assemblage consisted of a $BaCO_3$ tube as pressure medium, a graphite heater and crushable alumina also as pressure medium. The

diffusion couple was placed in the center of the heater so that the interface was at the hottest point of the assemblage. Temperature was measured on top of the sample at a distance of about 2.5 mm from the interface using a type-D thermocouple. Temperature at the interface was calculated assuming a gradient of 8°C/mm as determined by Zhang et al. [21] for a similar setup. Due to the relatively large distance between thermocouple and diffusion region, the accuracy of the sample temperature probably is not better than 20°C. The pressure uncertainty of the PCA is not exactly known, and is roughly estimated to be 50 MPa.

4. Analytical techniques

After each experiment, a slice was sectioned parallel to the diffusion direction near the center of the sample. The slice was polished on both surfaces to a typical thickness of 0.2–0.5 mm for electron microprobe and infrared (IR) measurements.

4.1. Electron microprobe analysis

The bulk composition of the glasses was determined by electron microprobe CAMECA CAMEBAX using 15 kV accelerating voltage and 18 nA beam current. To minimize alkali loss, the electron beam was defocused to 20–30 μm with counting times of 2 s on peak for Na and K and 5 s on peak for other elements. Compositions of hydrated and anhydrous glasses agree within analytical error if calculated on a water-free basis.

Ar was measured separately using a fixed matrix composition for calculating the Ar concentration in the glass. Analytical conditions were: 15 kV accelerating voltage, 140 nA beam current, 30 s counting time on the peak and 15 s on the background. The standard was a silica glass containing 1.0 wt% Ar as determined by gas chromatography (K. Roselieb, personal communication). Long profiles obtained in diffusion couple experiments at high T usually were measured using a beam defocused to 5–10 μm. To analyze short profiles of sorption experiments at low T the beam was focused to 1–2 μm. Tests with both dry and hydrous glasses show that counting rates of Ar are stable at these conditions. Ar concentrations determined using either a focused or a defocused beam do not differ by more than a few percent.

4.2. IR spectroscopy

H_2O, OH and total water concentrations were determined from IR spectra. A bulk spectrum of each hydrous glass cylinder was measured in the main chamber of a Fourier transform IR (FTIR) spectrometer (Bruker IFS88) before the experiment. Samples were mounted on a hole aperture with 1 mm in diameter to analyze the central volume of the cylinder. Profiles of water species and total water after the experiments were measured with an IR microscope A590 connected to the FTIR spectrometer. A slit aperture between the objective and the detector was used to limit the analysis sample volume. In the focal plane the area selected by the slit was typically 20 μm wide and 100 μm long resulting in a spatial resolution of about 30 μm (depending on the sample thickness). The sample was moved by a manually adjusted translation stage.

H_2O and OH concentrations were determined from the peak height of the absorption bands at 5230 cm^{-1} and 4520 cm^{-1}, respectively. At water contents >2 wt%, the calibration of Withers and Behrens [22] is used for the calculation of H_2O, OH and total water concentrations in rhyolitic glasses. This calibration is only established to be accurate at water contents 2–10 wt%. At lower water contents we applied the method of Zhang et al. [16]. For hydrous albitic glasses the calibration of Behrens et al. [23] was applied to evaluate the near-IR spectra. The water content of the 'dry' albitic glass was determined from the peak height of the mid-IR band at 3550 cm^{-1} to be 0.036 wt% [24].

5. Results

5.1. Ar sorption in water-poor melts

All samples obtained in Ar sorption experi-

ments were bubble-free. Major crystallization occurred in one experiment at 1000°C and 500 MPa using a rhyolitic glass containing 0.12 wt% water. In this particular experiment, the P–T conditions probably were too close to the liquidus of granitic melts [25]. This sample was not considered in the diffusion study. All other samples showed either no or only minor crystallization.

During Ar sorption experiments at ≥ 1000°C the edges of the wafers became rounded and the sample thickness increased by up to 20%. The increase of thickness was similar in three experiments using rhyolitic glasses at 500 MPa and 1000–1034°C, although run duration varied by a factor of 8. We therefore infer that the sample shape changed mainly at the beginning of the experiment. Further, Ar diffusion coefficients derived from these experiments agree within experimental error if the slightly different temperatures are taken into account. Therefore, convection did not significantly affect these profiles.

Ar profiles were evaluated assuming a constant density of the glass, a constant surface concentration $C_{0,\mathrm{Ar}}$ and a concentration-independent diffusion coefficient D_{Ar}. If the initial concentration of Ar in the glass is zero, the solution of Fick's second law for one-dimensional diffusion is [26]:

$$C_{\mathrm{Ar}} = C_{0,\mathrm{Ar}}\mathrm{erfc}\frac{x}{\sqrt{4D_{\mathrm{Ar}}t}} \quad (1)$$

where C_{Ar} is the concentration of Ar at the distance x from the surface and t is the run duration. To fit the profiles, $C_{0,\mathrm{Ar}}$ and D_{Ar} were adjustable parameters. $C_{0,\mathrm{Ar}}$ can be interpreted as the equilibrium solubility of Ar at the experimental conditions. For temperatures below 1000°C, fitted values of $C_{0,\mathrm{Ar}}$ are in good agreement with Ar concentrations directly measured by microprobe on the surface exposed to argon. In the high temperature experiments, the surfaces of the diffusion samples were altered and a reliable analysis was not possible by microprobe (see discrepancies between fitted and measured values of $C_{0,\mathrm{Ar}}$ in Table 2). A detailed analysis of the Ar solubility is out of the scope of the present study and, especially in the runs below 900°C, the profiles may be too short to enable a reliable determination of $C_{0,\mathrm{Ar}}$.

The Ar profiles of all experiments using starting glasses with less than 1 wt% water are well fitted by Eq. 1. Even the run with rhyolitic glass at 1102°C shows no systematic deviation between the data points and the fitted curve, although the temperature is far beyond the glass transition (T_g defined as the temperature at which the viscosity equals 10^{12} Pa s is 665°C for rhyolitic glass with 0.2 wt% water [27]). This supports the conclusion that Ar sorption still is controlled by diffusion at this temperature and that flow of the sample during the experiment has no significant influence on Ar transport into the glass.

In sorption runs except for Rhy-D12P the variation of water contents along the Ar profile is less than 0.5 wt%. Such a small variation does not produce a significant deviation of the Ar profile from simple error function shape. For experi-

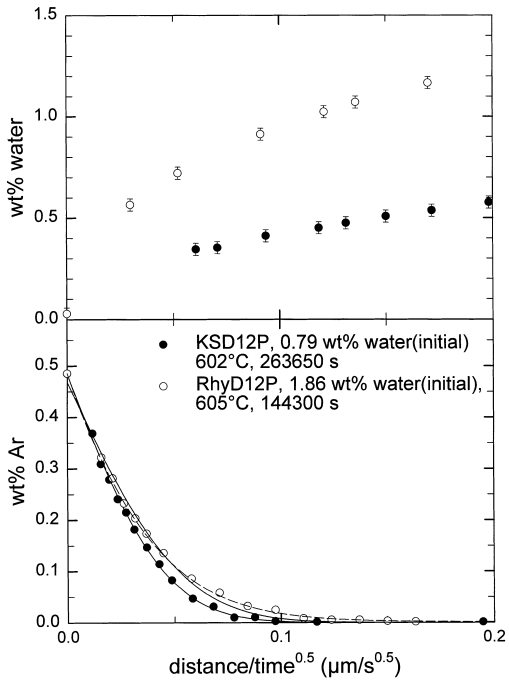

Fig. 1. Concentration–distance profiles for H_2O and Ar in rhyolitic glasses after Ar sorption experiments at 500 MPa. Solid lines are fits to the Ar profiles by Eq. 1. Note the deviation of data points from the fit at high normalized distances for the water-rich sample (Rhy-D12P). This effect is caused by the increase of Ar diffusivity with water content. By incorporating the dependence of Ar diffusivity on water content the Ar profile of Rhy-D12P can be fitted well (dashed curve).

ment Rhy-D12P, the initial water content is 1.86 wt%, and the variation of water content across the Ar profile is 0.9% (Fig. 1). The Ar profile shows a small but noticeable systematic deviation from the error function fit. That is, our Ar data (at high Ar concentrations) are precise enough to resolve small deviation from the error function shape and small diffusivity variations. Based on the dependence of D_{Ar} on water content derived later (Eq. 7), the variation of D_{Ar} across the profile is about a factor of 2.5 for the profile of Rhy-D12P (from water content of 0–0.9 wt%). Incorporating this dependence, the Ar concentration profile can be fitted very well (dashed curve in Fig. 1).

5.2. Diffusion couples with hydrous melts

Assuming concentration-independent diffusion coefficients, the solution of Fick's second law for one-dimensional diffusion between two semi-infinite media is [26]:

$$C_{Ar} = C_{0,Ar} + \frac{C_{1,Ar} - C_{0,Ar}}{2} \mathrm{erfc} \frac{x}{\sqrt{4 D_{Ar} t}} \quad (2)$$

where $C_{0,Ar}$ and $C_{1,Ar}$ are the initial concentrations in both halves of the diffusion couple. Eq. 2 was fitted to the measured concentration–distance profiles of Ar. An adjustable parameter beside the $C_{0,Ar}$, $C_{1,Ar}$ and D_{Ar} was the zero point of distance axis. The zero point so obtained corresponds to the Matano interface.

The measured Ar profiles when water concentration is constant can be fitted well with a constant D_{Ar} (Fig. 2a). In some experiments (e.g. DCRhyAr4-x, DCRhyAr3-3) two halves with different initial water contents were coupled so as to determine the concentration-dependent diffusion coefficient of Ar in a single experiment using a Boltzmann–Matano analysis [28]. However, because of the scatter of the data points due to

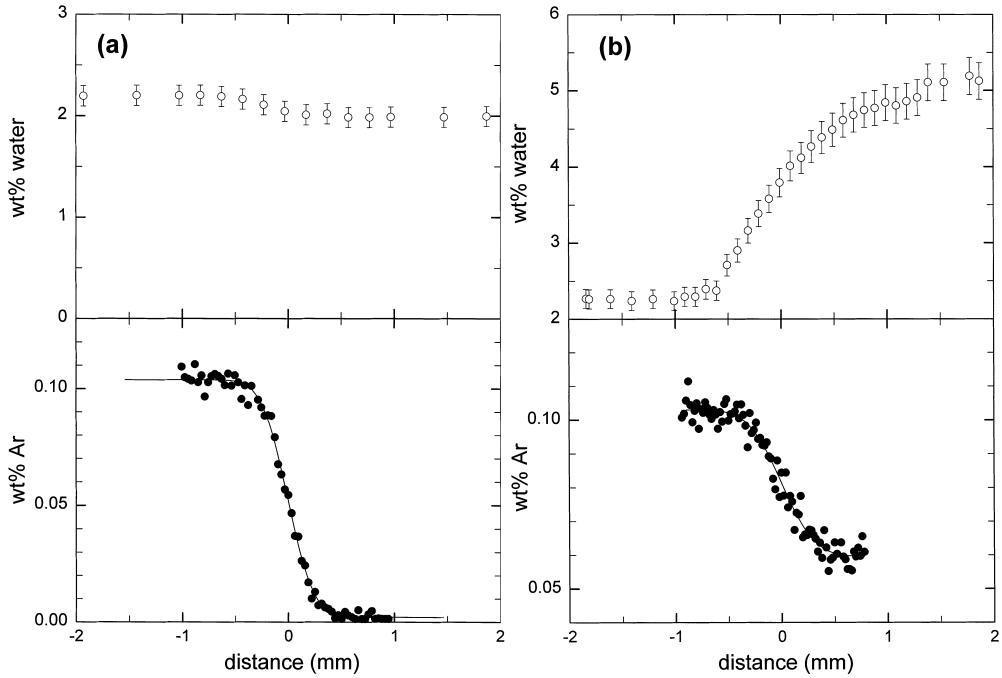

Fig. 2. Ar diffusion couple experiments with hydrous rhyolitic melts. Solid lines are fits to the Ar profiles by Eq. 2. The zero point of the x-axis is obtained from fitting the profiles. (a) Run DCRhyAr4-2 performed in an IHPV at 1102°C and 500 MPa for 1800 s. (b) Run DCRhyAr3-1 performed in an IHPV at 1034°C and 500 MPa for 5400 s. Note that despite the large initial difference in water content of the two halves, the Ar profile is well fitted assuming a constant Ar diffusivity.

low Ar concentrations, it is not possible to resolve the variation of D_{Ar} on water content from these profiles (Fig. 2b). The profiles show no significant misfit to Eq. 2 and the obtained averaged diffusion coefficient of Ar corresponds well to the water concentration at the interface.

5.3. Uncertainty in diffusion coefficients

A major uncertainty in the low temperature Ar sorption experiments is the position of the surface. Edges are slightly rounded or rough due to polishing. Hence the position of the original diffusion surface (which is the zero point of the distance axis after sectioning) cannot be exactly determined from backscattered electron images. We estimate the uncertainty of the surface position to be ± 2 μm. For short diffusion profiles, the resulting relative error of diffusivity can be large, 32% for experiments KS-D24P (480°C and 500 MPa) and KS-D23P (563°C, 500 MPa) and 11% for KS-D18P (592°C, 810 MPa). Slight deviation of the measured profile from the diffusion direction has only a minor influence on diffusion data. For example, if the measured profile is 10° off the diffusion direction, the corresponding increase of D_{Ar} only is 3%.

Another uncertainty is related to the presence of bubbles in diffusion couple experiments at 500 MPa (samples from runs at higher pressure were bubble-free). Size, concentration and distribution of the bubbles in the 500 MPa glasses appear to be unchanged compared to presumably air bubbles in the starting glasses. The length of Ar profiles in diffusion couples ranges from 140 to 660 μm, much longer than the diameter of the bubbles (10–20 μm). Because the bubbles are not interconnected and the volume is small, rapid Ar diffusion in the bubbles is not expected to significantly enhance transport of argon. On the other hand, because some Ar flux ended up in the bubbles, Ar diffusivities that we obtained might underestimate the true fluxes and diffusivities. The Ostwald solubility coefficient of Ar in rhyolitic melt at 500–1500 MPa is about 0.01 or greater [2] and for Ar mass in the bubbles to be the same as, or more than that in the melt would require a volume fraction of $\geq$1% for the bubbles. Because the bubble volume fraction is 0.1–0.2%, the Ar mass in the bubbles is about 10–20% of that in the melt. Hence diffusivity determined from the concentration profiles may underestimate the true diffusivity by at most 30%.

Uncertainty in pressure has no significant influence on the diffusion data because of the relatively small pressure dependence of Ar diffusivity. On the other hand, uncertainty in temperature has a larger effect. Based on an activation energy of 157 kJ/mol for Ar diffusion, the uncertainty of ± 10°C in temperature corresponds to errors in D_{Ar} of 30% at 500°C and 8% at 1200°C. In the low-T runs using CSPV, the duration is long compared to heating and cooling and no time correction is required. For all high-T runs, an effective run duration considering heating and cooling was calculated as outlined by Zhang and Behrens [1] assuming an activation energy for Ar diffusion of 157 kJ/mol. Only for the experiments in IHPV shorter than 90 min do heating and cooling contribute more than 1% to the effective run duration (Table 2). For sorption experiments, the Ar diffusivity is the average across a range of water contents. Hence a further source of error is the assignment of water content to an average Ar diffusivity. This water content is estimated to be that corresponding to the middle concentration of the Ar profile. The error is estimated to be less than one half of this water content. In the diffusion couple experiments, the water content at which the Ar diffusivity is determined is that at the inflection point of the Ar profile. The uncertainty of water concentrations is estimated by comparison to water concentration at distances of $\pm 2(D_{Ar}t)^{1/2}$ from the inflection point. Errors of the diffusion coefficients based on these estimates are included in Table 2.

6. Discussion

6.1. Ar diffusion in water-poor and hydrous melts

Diffusion data for water-poor rhyolitic glasses are in excellent agreement with data from Carroll [4] if differences in run pressure are taken into account (Fig. 3). The data obtained for rhyolitic

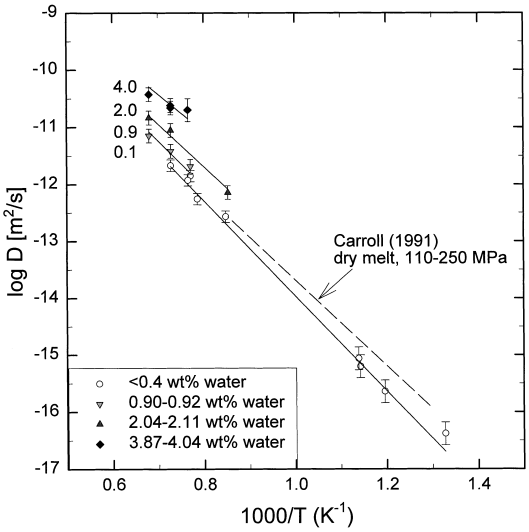

Fig. 3. Arrhenius plot for Ar diffusion in rhyolitic glasses and melts. Solid lines are calculations by Eq. 7 for 500 MPa and water contents (in wt%) as indicated. Data obtained by Carroll [4] for a melt containing 0.17% initial water are shown for comparison.

composition at 500 MPa can be described in the whole temperature range of 480–1102°C by a simple Arrhenius relationship:

$$D_{Ar} = D_0 \exp(-E_a/RT) \quad (3)$$

where D_0 is the pre-exponential factor and E_a is the activation energy for diffusion. The fitted values are log $D_0 = -5.67 \pm 0.21$ (D_0 in m^2/s) and $E_a = 157 \pm 4$ kJ/mol. These values are consistent with previous data of Carroll [4] at 110–250 MPa (log $D_0 = -6.16$ where D_0 is in m^2/s; $E_a = 144$ kJ/mol). Ar diffusion in albitic melts at 903 and 1015°C is faster than expected from previous studies [4,6] whereas data at 605°C are in good agreement. We do not have enough data to derive accurately an Arrhenius equation for Ar diffusion in albitic melt.

The effect of dissolved water on Ar diffusivity is similar for albitic and rhyolitic melts. Adding 4 wt% water to the dry melt at 1000°C and 500 MPa increases D_{Ar} by about one order of magnitude. In the range 0.1–5 wt% water, D_{Ar} depends

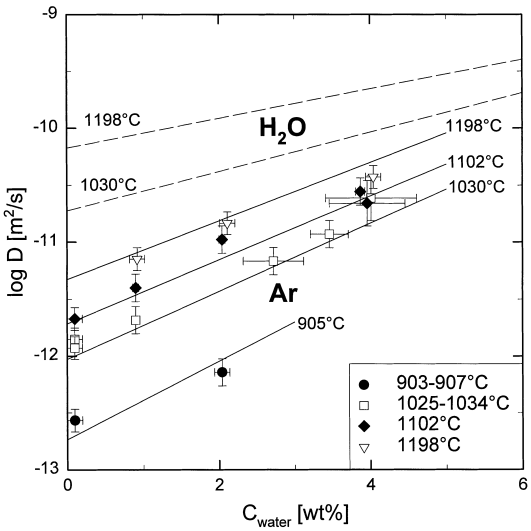

Fig. 4. Dependence of Ar diffusion in rhyolitic melts on dissolved water. Solid lines are fits by Eq. 7. Diffusivity of molecular H_2O (dashed lines) is calculated after Zhang and Behrens [1].

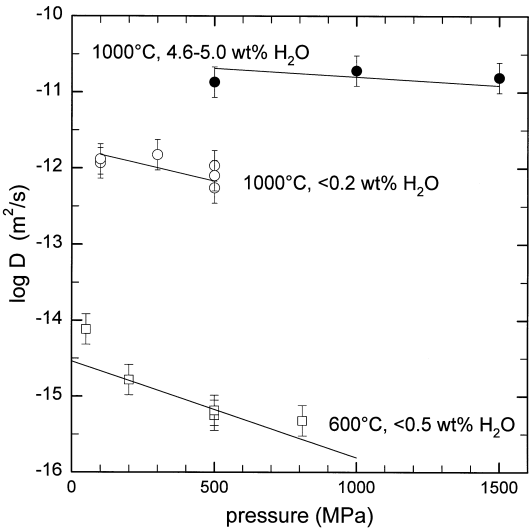

Fig. 5. Pressure dependence of Ar diffusion in rhyolitic glasses/melts. Experimental data are corrected for small deviations in temperature. The deviation between calculated diffusivity (solid line) at 600°C and the experimental data at low and high pressure may indicate a pressure dependence of the activation volume which is not considered in the simplified fit approach.

exponentially on water content at temperatures from 900 to 1200°C (Fig. 4).

6.2. Pressure dependence of Ar diffusivity

At 600°C Ar diffusivity in water-poor rhyolitic glasses strongly decreases with pressure from 7.7×10^{-15} m^2/s at 50 MPa to 4.8×10^{-16} m^2/s at 810 MPa (Fig. 5). The data seem to indicate a non-linear variation of Ar diffusivity with pressure at 600°C. However, the error of the low-T data is too large and the number of experiments is too small to prove non-linearity. For simplicity we use the convenient relation:

$$D_{\mathrm{Ar}} = D_{0'} \exp(-PV/RT) \tag{4}$$

to describe the pressure dependence of diffusivity, where $D_{0'}$ is the diffusivity at 1 bar and V is the activation volume. The average activation volume in the range 200–810 MPa is 15 ± 5 cm^3/mol. At 1000°C the effect of pressure on D_{Ar} is relatively small compared to the experimental error. The derived activation volume of 13 ± 7 cm^3/mol is close to the value obtained at low temperature, indicating that the activation volume is not sensitive to temperature. However, it is emphasized that the range of pressures and the number of experiments is too small to allow an accurate quantification of the activation volume. Our value for the activation volume for Ar diffusion in water-poor rhyolitic melts is significantly smaller than the value of 36 cm^3/mol at 800°C determined by Carroll [4] for rhyolitic melts (the pressure range is very small, from 136 to 370 MPa, in [4]) but it agrees well with the value of 11.4 cm^3/mol determined for Ar diffusion in jadeite melts [8]. Our result of the activation volume for Ar diffusion is similar to the atomic volume of Ar (11.1 cm^3/mol assuming atoms as spheres [30]).

For rhyolitic melts containing 4.6–5.2 wt% water the pressure dependence of D_{Ar} is negligible. An activation volume of only 1 cm^3/mol is derived from the three PCA experiments at pressures from 500 to 1500 MPa. It is noteworthy that the viscosity of hydrous silicic melt is also insensitive to pressure [30].

6.3. Modeling Ar diffusion as a function of T, P and X_{water}

Combining Eqs. 3 and 4 yields an equation of the following type:

$$D_{\mathrm{Ar}} = \exp(a_0 + a_1/T + a_2P/T) \tag{5}$$

The parameters a_0, a_1 and a_2 are related to the pre-exponential factor, the activation energy and the activation volume, respectively. Ar diffusivity varies exponentially with water concentration, but the compositional variation may be dependent on pressure and temperature. The simplest expression accounting for this is:

$$D_{\mathrm{Ar}} = \exp[(a_0 + b_0X_{\mathrm{water}}) + (a_1 + b_1X_{\mathrm{water}})/T + (a_2 + b_1X_{\mathrm{water}})P/T] \tag{6a}$$

or:

$$D_{\mathrm{Ar}} = \exp[(a_0 + a_1/T + a_2P/T) + (b_0 + b_1/T + b_2P/T)X_{\mathrm{water}}] \tag{6b}$$

where X_{water} is the mol fraction of water in the melt on a single oxygen basis. The parameters a_0, a_1, a_2, b_0, b_1, and b_2 are to be obtained by fitting experimental data to Eqs. 6a and 6b. Combining our data with the data of Carroll [4], preliminary fitting indicates that b_0 is indistinguishable from zero. Refitting by letting $b_0=0$, the following equation was obtained for Ar diffusivity (in 10^{-12} m^2/s) in rhyolitic melts as a function of pressure (in MPa), temperature (in K) and mol fraction of water:

$$D_{\mathrm{Ar}} = \exp[(14.627-17913/T-2.569P/T) + (35936/T + 27.42P/T)X_{\mathrm{water}}] \tag{7}$$

This equation is based on 36 data for water-poor melts and 14 data for hydrous melts. The standard error of estimate is 0.29 for ln D_{Ar}. Except for two outlier points (500 and 800°C data of Carroll [4]) with error of estimates ranging from 0.6 to 0.7 on ln D, the error of estimates is ≤ 0.46

in terms of ln D for all other data. However, it is emphasized that there are no data for hydrous melts at temperatures below 900°C, because samples rapidly crystallized at such conditions. Thus, caution should be exercised to apply Eq. 7 to model low temperature processes in hydrous magmas, e.g. magma degassing (although we expect that extrapolation to 800°C would not generate large errors). Moreover, our simple approach does not consider a variation of activation volume with pressure (see Fig. 5). To model Ar diffusion more precisely, additional parameters are required to account for possible pressure and temperature dependence of activation volume and energy. Such parameters are poorly constrained by the available data.

From the above equation, the dependence of Ar diffusion in rhyolitic melts on water content is more pronounced at low than at high temperatures (see Fig. 4). Further, the activation energy for Ar diffusion in water-poor rhyolitic melts increases with pressure from 149 kJ/mol at 0.1 MPa to 160 kJ/mol at 500 MPa. Adding 4 wt% water to the melt at 500 MPa decreases E_a to 121 kJ/mol. The pressure dependence of Ar diffusivity is more pronounced at low water content than at high water content.

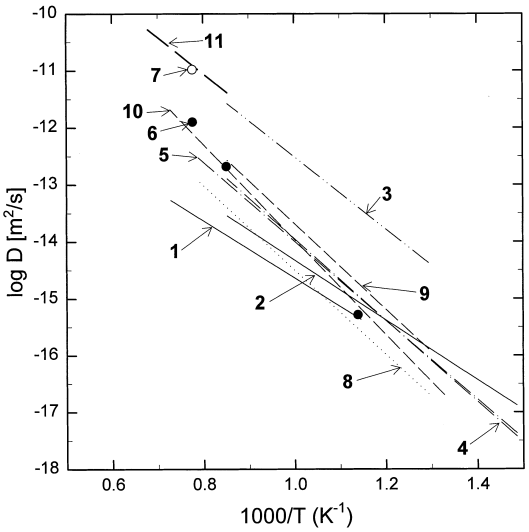

Fig. 6. Ar diffusion in silica-rich melts. Data sources: 1: SiO_2, dry, 1 atm desorption kinetics [7]; 2: SiO_2, dry, 20–375 MPa, profiling [5]; 3: $KAlSi_3O_8$, dry, 130–240 MPa, profiling [4]; 4: $NaAlSi_3O_8$, dry, 1 atm, desorption kinetics [6]; 5: $NaAlSi_3O_8$, dry, 110–250 MPa, profiling [4]; 6: $NaAlSi_3O_8$, dry, 500 MPa, profiling, this study; 7: $NaAlSi_3O_8$, 4 wt% H_2O, 500 MPa, profiling, this study; 8: $NaAlSi_2O_6$, dry, 1 atm, desorption kinetics [7]; 9: rhyolite, water-poor, 110–250 MPa, profiling [5]; 10: rhyolite, 0.1 wt% H_2O, 500 MPa, profiling, this study; 11: rhyolite, 4 wt% H_2O, 500 MPa, profiling, this study.

6.4. Comparison with Ar diffusivity in other silica-rich melts

Experimental data for Ar diffusion in various silica-rich melts are compared in Fig. 6. Data for rhyolitic, albitic and jadeitic melts cover a narrow range in the Arrhenius diagram. Ar diffusivity in $KAlSi_3O_8$ melts is faster by one order of magnitude compared to the other melts. A possible explanation for this is the more open structure and the lower density of Or glass, a reflection of the larger size of K compared to Na [4]. Ar diffusivity in hydrous rhyolitic and albitic melts with 4 wt% water is very similar to that in dry Or melts, supporting this idea because the density of glasses decreases by incorporation of the light H_2O component [31]. However, if diffusivity is controlled only by the density of packing atoms in the glass structure, one would expect a fast diffusion of Ar in silica glass too. This is not the case. At temperatures below 800°C, Ar diffusivity in silica glass is similar to that in dry rhyolitic, albitic and jadeitic glasses. At higher temperatures, Ar becomes increasingly less mobile in silica glass compared to the other compositions, due to the low activation energy for Ar diffusion in silica glass. Hence, we infer that Ar diffusivity is not a simple function of composition, although composition-related structural differences do play an important role.

6.5. Implications for diffusion of other volatiles

Fig. 7 compares diffusion of various cations and volatiles to 'Eyring diffusivity' calculated from viscosity data using the Eyring equation. At 800°C, diffusivity of the volatiles Ar, CO_2 and H_2O in rhyolitic melts is three to four orders of magnitude greater than 'Eyring diffusivity'. A jumping distance of 0.03 pm has to be assumed for these volatiles if their motion is controlled by

melt viscosity. A large effect of water on diffusivity is observed for all diffusing species except the mobile Na cation.

6.5.1. H_2O

In a previous paper, a model for water diffusion in rhyolitic melt was developed assuming an exponential dependence of diffusivity of molecular H_2O on water content and negligible diffusivity of OH groups [1]. The model accurately reproduces the concentration–distance profiles for total water measured after diffusion couple experiment with rhyolitic melts. Our new Ar diffusion data as well as the CO_2 diffusion data of Watson [11] show that assuming an exponential variation with water content is valid for diffusion of uncharged particles (such as H_2O molecules) in rhyolitic melts. Lower diffusivities (see Fig. 4) and lower activation energies for H_2O diffusion than for Ar diffusion (e.g. 122 kJ/mol for Ar and 83 kJ/mol for H_2O molecules at 500 MPa and 4 wt% water) are consistent with the smaller size of H_2O molecules compared to Ar atoms [29]. Quantitative effect of dissolved water on diffusion of charged species (such as Cs^+) may depend on charge balance and speciation, and hence can be more complicated.

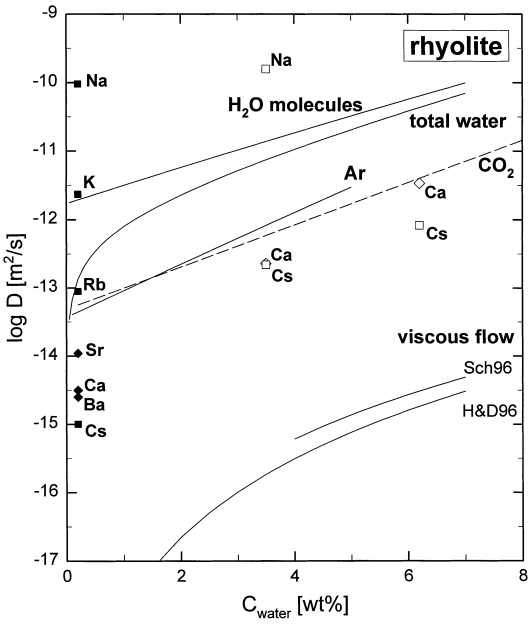

Fig. 7. Comparison of various diffusion processes in rhyolitic melts at 800°C. Data sources: total water and molecular H_2O at 500 MPa [1], Ar at 500 MPa, extrapolated from this study, CO_2 in water-poor melts at 50–105 MPa [33], CO_2 in hydrous melts at 1000 MPa [11], Na, K, Rb, Cs, Ca in water-poor glasses at 1 atm [3], Sr, Ba in water-poor glasses at 1 atm [35], Na, Cs, Ca in hydrous glasses [11], chemical diffusivities were calculated by the Eyring equation assuming a jump distance of 0.3 nm using the viscosity models of Hess and Dingwell [27] and Schulze et al. [30].

6.5.2. CO_2

The diffusivities of CO_2 and Ar are almost identical in water-poor rhyolitic melts over a wide range of temperatures and pressures [11,32,33]. Furthermore, comparison of our results for Ar diffusion with data for CO_2 diffusion from Watson [11] shows a similar dependence on water content for both volatiles (Fig. 7). IR spectroscopy gives evidence that CO_2 molecules are the dominant carbon dioxide species in rhyolitic glasses [34]. There is no indication of the presence of carbonate groups from the spectra. CO_2 is a long cylindrical molecule with a base radius of 1.4 Å and a half-length of about 2.5 Å, and Ar atoms are spherical with a radius of 1.64 Å [29]. The similarity between Ar and CO_2 diffusivity implies that a smaller base radius compensates the greater half-length of the CO_2 molecule and that the linear CO_2 molecule moves as an oriented molecule to minimize expansion of the doorways of the silicate network. In water-poor rhyolites diffusion of Ar and CO_2 is similar to Rb^+ (radius 1.52 Å) indicating that the effect of the smaller radius of the Rb^+ cation (compared to Ar) to increase the diffusivity is compensated by the need to balance the charge because increasing charge typically reduces the mobility of particles (atoms or cations) in silicate melts.

6.6. *Implication for fractionation of volatiles during degassing of magmas*

During magma degassing, there are three possible fractionation processes. One is equilibrium fractionation owing to different solubilities of the gases, which occurs if the degassing process is slow so that equilibrium between the bubbles and the bulk melt is reached. The second is frac-

tionation during dynamic degassing when bubbles are removed once they form, resulting in Rayleigh fractionation. The third is kinetic fractionation owing to different diffusivity of the gases in the melt, which occurs if the degassing process is rapid so that only the melt at the bubble surface is in equilibrium with the bubbles. To model equilibrium and dynamic fractionation, diffusion can be ignored. To model kinetic fractionation, both surface equilibrium and diffusion must still be considered.

Coupled H_2O, CO_2, N_2 and noble gas investigations in melts have the potential to reveal the details of the degassing process because different controls can be distinguished. In rhyolitic melt, Ar and CO_2 have similar Ar diffusivity (Fig. 7) and similar molar solubility. Hence the Ar/CO_2 ratio would not be much fractionated by either equilibrium or dynamic or kinetic fractionation. Kr and CO_2 solubilities are similar (Kr solubility is 30% less than CO_2 solubility [2]) but Kr diffusivity is about two orders of magnitude smaller [36]. Hence significant fractionation in the Kr/CO_2 ratio would indicate kinetic control in degassing. Quantitative modeling for kinetic fractionation can also be developed when the relevant data for such applications are available.

Acknowledgements

This research is supported by NSF Grants INT-9815351 and EAR-9972937 and by the German DAAD. We thank S. Chakraborty, D. Draper and an anonymous third reviewer for their constructive and insightful comments.***[BW]***

References

[1] Y. Zhang, H. Behrens, H_2O diffusion in rhyolitic melts and glasses, Chem. Geol. 169 (2000) 243–262.

[2] M.R. Carroll, J.D. Webster, Solubilities of sulfur, noble gases, nitrogen, chlorine, and fluorine in magmas, Rev. Mineral. 30 (1994) 231–279.

[3] A. Jambon, Tracer diffusion in granitic melts: Experimental results for Na, K, Rb, Cs, Ca, Sr, Ba, Ce, Eu to 1300°C and a model for calculation, J. Geophys. Res. 87 (1982) 10797–10810.

[4] M.R. Carroll, Diffusion of Ar in rhyolite, orthoclase and albite composition glasses, Earth Planet. Sci. Lett. 103 (1991) 156–168.

[5] M.R. Carroll, E.M. Stolper, Argon solubility and diffusion in silica glass: Implications for the solution behavior of molecular gases, Geochim. Cosmochim. Acta 55 (1991) 211–225.

[6] K. Roselieb, W. Rammensee, H. Büttner, M. Rosenhauer, Solubility and diffusion of noble gases in vitreous albite, Chem. Geol. 96 (1992) 241–266.

[7] K. Roselieb, W. Rammensee, H. Büttner, M. Rosenhauer, Diffusion of noble gases in melts of the system SiO_2–$NaAlSi_2O_6$, Chem. Geol. 120 (1995) 1–13.

[8] K. Roselieb, H. Büttner, U. Eicke, U. Köhler, M. Rosenhauer, Pressure dependence of Ar and Kr diffusion in a jadeite melt, Chem. Geol. 128 (1996) 207–216.

[9] M.C. Johnson, A.T. Anderson Jr., M.J. Rutherford, Pre-eruptive volatile contents of magmas, Rev. Mineral. 30 (1994) 281–330.

[10] E.B. Watson, Diffusion in magmas at depth in the Earth: The effects of pressure and dissolved H_2O, Earth Planet. Sci. Lett. 52 (1981) 291–301.

[11] E.B. Watson, Diffusion of dissolved CO_2 and Cl in hydrous silicic to intermediate magmas, Geochim. Cosmochim. Acta 55 (1991) 1897–1902.

[12] J. Koepke, H. Behrens, Trace element diffusion in andesitic melts – an application of synchroton X-ray fluorescence analysis, Geochim. Cosmochim. Acta 65 (2001) 1481–1498.

[13] R.H. Doremus, Glass Science, Wiley, New York, 1973, 379 pp.

[14] Y. Zhang, E.M. Stolper, G.J. Wasserburg, Diffusion of water in rhyolitic glasses, Geochim. Cosmochim. Acta 55 (1991) 441–456.

[15] H. Behrens, M. Nowak, The mechanisms of water diffusion in polymerized melts, Contrib. Mineral. Petrol. 126 (1997) 377–385.

[16] Y. Zhang, R. Belcher, P.D. Ihinger, L.P. Wang, Z.J. Xu, S. Newman, New calibration of infrared measurement of dissolved water in rhyolitic glasses, Am. Mineral. 80 (1997) 593–612.

[17] A.C. Withers, Y. Zhang, H. Behrens, Reconcilation of experimental data on water speciation in rhyolitic glass using in situ and quenching techniques, Earth Planet. Sci. Lett. 173 (1999) 343–351.

[18] Y. Zhang, H_2O in rhyolitic glasses and melts: measurement, speciation, solubility, and diffusion, Rev. Geophys. 37 (1999) 493–516.

[19] S. Ohlhorst, H. Behrens, F. Holtz, B.C. Schmidt, in: D. Rammlmair, J. Mederer, Th. Oberthür, R.B. Heimann, H. Pentinghaus (Eds.), Applied Mineralogy in Research, Economy, Technology and Culture, Proc. 6th Int. Conf. Appl. Mineral., Balkema, Rotterdam 1, 2000, pp. 193–196.

[20] Y. Zhang, Z. Xu, H. Behrens, Hydrous species geospeedometer in rhyolite: improved calibration and application, Geochim. Cosmochim. Acta 64 (2000) 3347–3355.

[21] Y. Zhang, D. Walker, C.E. Lesher, Diffusive crystal dissolution, Contrib. Mineral. Petrol. 102 (1989) 492–513.
[22] A.C. Withers, H. Behrens, Temperature induced changes in the NIR spectra of hydrous albitic and rhyolitic glasses between 300 and 100 K, Phys. Chem. Minerals 27 (1999) 119–132.
[23] H. Behrens, C. Romano, M. Nowak, F. Holtz, D.B. Dingwell, Near-infrared spectroscopic determination of water species in glasses of the system $MAlSi_3O_8$ (M = Li, Na, K): an interlaboratory study, Chem. Geol. 128 (1996) 41–64.
[24] H. Behrens, M.O. Schmidt, Infrared spectroscopy of hydrous silicic glasses at temperatures up to 600°C and implications for the incorporation and dynamics of water in the glasses, N. Jahrb. Mineral. Abh. 172 (1998) 203–226.
[25] F. Holtz, W. Johannes, N. Tamic, H. Behrens, Maximum and minimum water contents of granitic melts generated in the crust: a reevaluation and implications, Lithos 46 (2001) 1–14.
[26] J. Crank, The Mathemathics of Diffusion, 2nd edn., Clarendon Press, Oxford, 1975, 414 pp.
[27] K.-U. Hess, D.B. Dingwell, Viscosities of hydrous leucogranitic melts: A non Arrhenian model, Am. Mineral. 81 (1996) 1297–1300.
[28] M. Nowak, H. Behrens, An experimental investigation on diffusion of water in haplogranitic melts, Contrib. Mineral. Petrol. 126 (1997) 365–376.
[29] Y. Zhang, Z. Xu, Atomic radii of noble gas elements in condensed phases, Am. Mineral. 80 (1995) 670–675.
[30] F. Schulze, H. Behrens, F. Holtz, J. Roux, W. Johannes, The influence of H_2O on the viscosity of a haplogranitic melt, Am. Mineral. 81 (1996) 1155–1165.
[31] P. Richet, A. Whittington, F. Holtz, H. Behrens, S. Ohlhorst, M. Wilke, Water and the density of silicate glasses, Contrib. Mineral. Petrol. 138 (2000) 337–347.
[32] J.G. Blank, E.M. Stolper, Y. Zhang, Diffusion of CO_2 in rhyolitic melt, Trans. Am. Geophys. Union 72 (1991) 312.
[33] H. Behrens, N. Tamic, Y. Zhang, F. Holtz, Diffusion of volatiles in rhyolitic melts: comparison of CO_2, Ar and molecular H_2O, Eur. J. Mineral. Beih. 12 (2000) 10.
[34] N. Tamic, H. Behrens, F. Holtz, The solubility of H_2O and CO_2 in rhyolitic melts in equilibrium with a mixed CO_2–H_2O fluid phase, Chem. Geol. 174 (2001) 333–347.
[35] M. Margaritz, A.W. Hofmann, Diffusion of Sr, Ba, and Na in obsidian, Geochim. Cosmochim. Acta 42 (1978) 595–605.
[36] M.R. Carroll, S.R. Sutton, M.L. Rivers, D.S. Woolum, An experimental study of krypton diffusion and solubility in silicic glasses, Chem. Geol. 109 (1993) 9–28.